CHAPTER 1

Introduction

Presently, the growing number of different organic pollutants can lead to worldwide problems. Thus it is urgent to develop possible techniques to eliminate environmental contaminations. For different organic pollutants, water soluble organic dyes as the main pollutants in water resources are needed to be treated. Wastewater from textile industries contains a considerable amount of dyes which may be carcinogenic and toxic to humans [1, 2]. Thus the development of an efficient and mild technology for removing organic dyes from wastewater is the prime challenge. Up until now, nanoscience and nanotechnology have been increasingly important for applications in wastewater treatment. A number of nanomaterials have been synthesized and used for the removal of pollutants in wastewater. Heterostructure nanomaterials including nanorods, nanoplates, nanotubes and nanocubes have been widely researched and studied on their properties relating to enhance photonic absorption, owing to their quantum confinement effect, high specific surface area, tunable surface to volume ratio and hierarchical porous structure. Nanomaterials have a large number of active sites to interact with different chemical species to obtain better results for the removal of pollutants from wastewater. Nanomaterials are now becoming new alternative ways for using as photocatalytic materials for wastewater treatment [3–5]. Different semiconducting nanomaterials have been reported to be applicable for the photodegradation of organic pollutants by transforming the materials into non–hazardous compounds under photonic illumination. These semiconductors are not costing a lot of money and can easily mineralize different organic compounds [6, 7].

Metal hydroxide as one of the most important family of functional materials can be used for a number of photocatalytic applications [8, 9]. Most of them possess hydroxyl (OH^-)

groups and terminal hydroxyl on surfaces [10]. Zinc hydroxystannate (ZHS) is a class of perovskite hydroxide with face–centered cubic close packed structure. It is nontoxic and high effective flame– and smoke– retardant properties [11–15]. The ZHS is an important functional nanomaterial with very highly efficient applications: lithium ion battery anodes [16–18], sensors [19, 20], solar cells [21] and photocatalysts [22–27]. The surface OH^- groups of ZHS play an important role in the photocatalytic process. These groups can accept photogenerated holes to form hydroxyl radicals ($\cdot OH$) which are active in photo–oxidation. The hydroxide surface is full of OH^- groups when it is excited by UV radiation. Thus the compound should have the efficiency for photoactivity [11].

There are a number of synthetic methods such as grinding [12], co–precipitation [12], sonochemical [10, 28–29], hydrothermal [25–27, 30–34] and solvothermal [11, 35] that have been developed to synthesize micro– and nano– crystalline ZHS with different shapes and sizes. Most of the resultant materials were aggregated, non–uniform in size, required high reaction temperature and long reaction time. Thus, it is highly desirable to find a low temperature, environmentally benign and convenient route for mass production of well disperse and uniform material. Microwave has been used for the synthesis of materials, including inorganic complexes, oxide and sulfide. The microwave has shown very rapid growth in different applications to materials science and engineering due to the unique reaction effect. The volumetric constant is rapidly heated up to high temperature by microwave within a very short time. Thus, the microwave method is very high interesting because shape and size of the materials are able to be controlled with ease even at different synthetic conditions [36–39].

In the present research, the synthesis of cubic–like $ZnSn(OH)_6$ particles in surfactant–free solution by a microwave method was reported. This method has the advantage for synthesis of homogeneous and nanosized particles because nucleation and crystalline growth proceeded at low temperature. Moreover, the method is expected to achieve low–dimensional particles, high yield, high crystalline degree, and able to apply for industrial scale synthesis. The as–synthesized compound was characterized by different techniques to determine phase, morphology, crystallite size, atomic vibration and optical properties. The best semiconducting material was used for photocatalytic study as well.

1.1 Properties of zinc hydroxystannate and its applications

1.1.1 Crystal structures

Zinc hydroxystannate (ZHS) is a class of typical perovskite–structured hydroxide compounds with the formula $MSn(OH)_6$ (M = bivalent metal atom), and belong to the ReO_3 class of materials having a three–dimensional structural framework. In this compound, the metal atoms are octahedrally coordinated with oxygen atoms to form $Sn(OH)_6$ and $Zn(OH)_6$ polyhedra, and these polyhedra share their “O” corners to build the structure frame–work. Furthermore, ZHS could be transformed into $ZnSnO_3$ or SnO_2/Zn_2SnO_4 mixture further thermal decomposition, which is known to have a two–stage thermal decomposition process [11–12]:

$$ZnSn(OH)_6 \longrightarrow ZnSnO_3 + 3H_2O$$

$$2ZnSnO_3 \longrightarrow Zn_2SnO_4 + SnO_2$$

The crystallographic $ZnSn(OH)_6$ and $ZnSnO_3$ are shown in Figure 1.1a and 1.1b, respectively. The framework of $ZnSn(OH)_6$ share their O–H in the corner–site of each polyhedral cell while that of $ZnSnO_3$ share their O in the same corner to built–in the framework of the $ZnSn(OH)_6$ and $ZnSnO_3$ crystal structure [40].

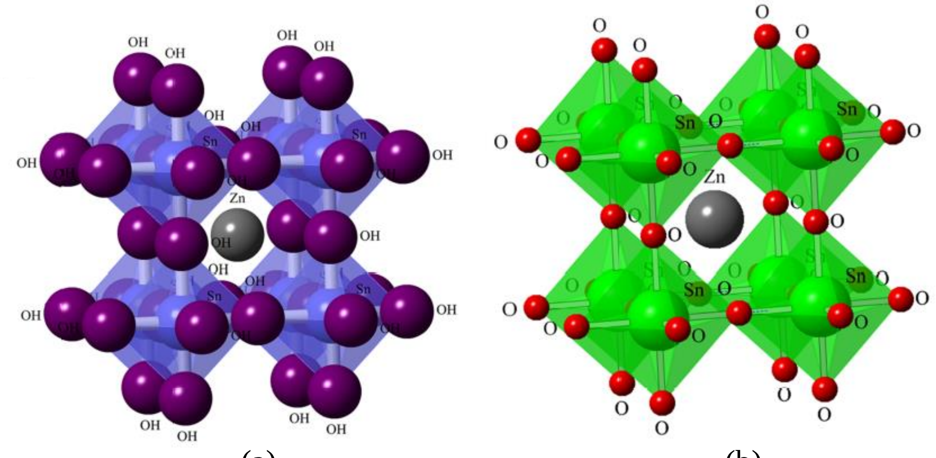

(a) (b)

Figure 1.1 Crystallographic structure of (a) $ZnSn(OH)_6$ and (b) $ZnSnO_3$ [40].

1.1.2 Toxicology

Zinc hydroxystannate is a very low toxicity. Due to its low acute oral, inhalation and dermal toxicity. Dust may irritate respiration system or lungs and prolonged contact may cause mild skin discomfort. Particles in the eye may cause irritation and redness. This compound is not considered carcinogenic by Occupational Safety and Health Administration (OSHA), International Agency for Research on Cancer (IARC), Nation Toxicology Program (NTP) and American Conference of Governmental Industrial Hygienists (ACGIH) [41].

1.1.3 Optical properties

ZHS is a wide band gap materials with band gap reported as 3.20–4.35 eV. It absorbs electromagnetic spectrum in ultraviolet region, which relates to wide band gap for the direct band gap semiconductor. The valence band top is completely dominated by the O 2p states, while the conduction band bottom mainly composes of the Sn 5s orbitals with minor contribution from the Sn 2p orbitals. The optical and electrical properties of ZHS were found to depend on its chemical composition, crystallinity and morphology, size and shape. ZHS that was synthesized by solvothermal method was normally microsphere, while hydrothermal and co–precipitation method have been used to synthesize nanoparticles ZHS. The band gap of microsphere ZHS was found to be 3.30 eV, which is much smaller than reported nanoparticles ZHS band gap (3.74–4.35 eV) [42].

1.1.4 Applications

Zinc hydroxystannate (ZHS) has a unique crystal structures of hydroxide compound. Due to its economical, environment–friendly, safety, and high effective flame– and smoke– retardant properties. ZHS has been widely used as a nontoxic flame retardant and smoke suppressant additive for many polymeric materials, anode materials for Li–ion batteries, gas sensors, dye-sensitized solar cells, and photocatalysts.

1) Flame retardant and smoke suppressant

Combinations of antimony are used commercially to flame retard flexible poly vinyl chloride (PVC) wire and cable formulations. This combination is effective in reducing the total amount of additives required to flame retard the formulation, reduce smoke generation, and minimize costs. Unfortunately, smoke–generation values for these formulations are increased if the antimony oxide content is increased. ZHS as one of the most important synergistic agent can be used for halogenated flame retardant additives and smoke suppressants. It is reported to be effective as either a full or partial replacement for antimony oxide in polymer containing halogenated flame retardants. ZHS is well documented as non–toxic flame retardant and smoke suppressant in a wide range of polymeric substrates, including halogenated polyesters, rigid and flexible PVC, chlorinated elastomers and in alkyd resin–based paint systems. The ZHS is more thermally stable and is used in polymers processed at temperatures above 200 ºC. Another advantage of this formulation is that it produces less smoke than those using antimony oxide as a flame retardant synergist [13–15].

2) Anode materials for lithium ion batteries

The most attractive tin–based ternary oxide ZHS has been widely investigated as an anode materials for Li–ion batteries due to low cost, ready availability and ecofriendly. It exhibited good electrochemical properties. Chen *et al.* [17] synthesized ZHS nanocube–graphene composite as an anode material for Li–ion batteries. It was found that these composites exhibited clearly improved electrochemical performance compared with bulk ZHS. Recently, Liu *et al.* [18] prepared ZHS nanocubes as anode electrode materials for Zn/Ni secondary battery which exhibited high electrochemical activities, including lower resistances and longer cycle life. These fascinating properties could be attributed to the Sn species can be reduced into Sn metal and it will form a highly conductive network, which is beneficial to improve the electrical contact between active material particles and diminish the polarization of the electrode.

3) Gas sensors

ZHS micro/nanostructures, being a wide band gap semiconductor is an appropriate material for application in gas sensor. This is because nanosized grains of metal oxides are almost depleted of carriers (most carriers are trapped in surface states) and exhibit much poorer conductivity than microsized grains in ambient air, hence, when exposed to target gases, they exhibit greater conductance changes as more carriers are activated from their trapped states to the conduction band than with microsized grains. The sensitivity of the electrical resistivity of ZHS to the gaseous formaldehyde (HCHO), ethanol (C_2H_5OH), carbon monoxide (CO) and benzene makes it potentially useful for sensing applications. Recently, Han *et al*. have been prepared ZHS microcrystallites with two morphologies, and the gas sensors based on ZHS presented a good sensor performance towards HCHO [19]. Liu *et al*. were successfully synthesized solid and hollow ZHS spheres, and gas sensor tests indicate that hollow ZHS spheres have a better response to ethanol [43].

1.2 Photocatalytic Activity

The acceleration of a chemical transformation by the presence of a catalyst with light is called photocatalytic. The catalyst may accelerate the photoreaction by interaction with the substrate in its ground or excited state and with a primary photoproduct, depending upon the mechanism of the photoreaction and itself remaining unaltered at the end of each catalytic cycle. Photocatalytic processes may occur homogeneously and heterogeneously. Heterogeneous catalysts are distinguished from homogeneous catalysts by the different phases present during reaction. Homogeneous catalysts are present in the same phase as reactants and products, usually liquid, while heterogeneous catalysts are present in a different phase, usually solid. Metal salts of organic acids, organometallic complexes, and carbonyl of Co, Fe, and Rh are typical homogeneously photocatalyst. Typical heterogeneous photocatalysts are inorganic solids such as metals, oxides, sulfides, and metal salts, but they may also be organic materials such as organic hydroperoxides, ion exchangers, and enzymes. The main advantage of using a heterogeneous photocatalyst is the utilization of semiconductor for photochemical degradation of organic pollutants. Additionally, heterogeneous photocatalytic reaction involves adsorption of reactants from a fluid phase onto a solid surface, surface reaction of adsorbed species, and desorption of products into the fluid phase.

1.2.1 Semiconducting materials

Semiconductor materials have received much attention during last decades as a promising solution for both energy generation and environmental problems. These materials have special electronic and optical properties which are determined by the band structure. The bands of interest in photocatalysis are the populated valence band (VB) and it’s largely vacant conduction band (CB), which is commonly characterized by band gap energy (E_g). Solids with different band widths give distinct properties and they are classified as: metals, semiconductors and insulators as shown in Figure 1.2.

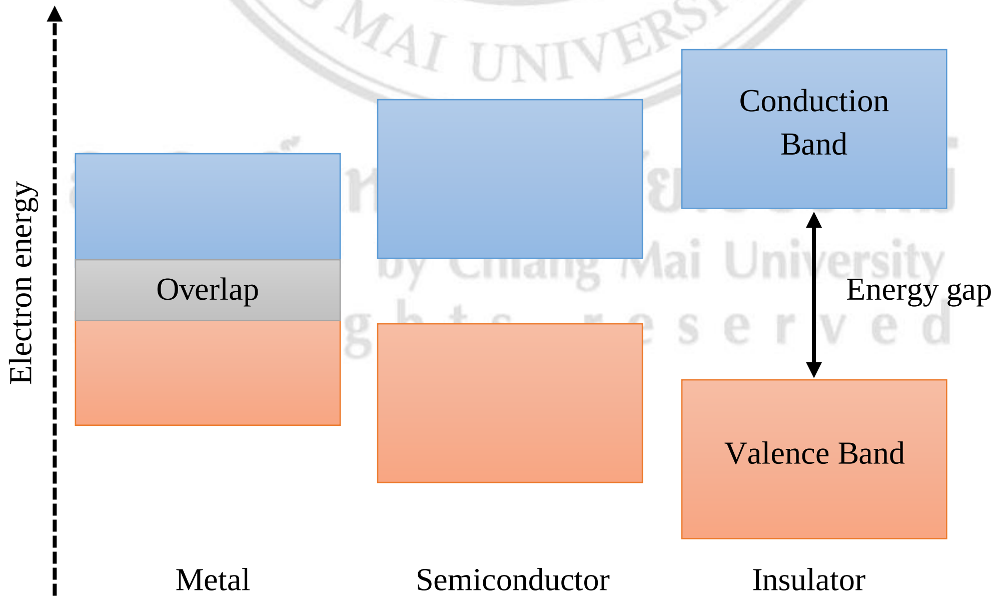

Figure 1.2 Comparison between the band gaps of metals, insulators and semiconductors [44].

When the band gap is overlapped, solids behave like metal (conductor) and regardless of temperature. Between the band gaps, higher band is called conduction band because only when electrons are excited to the conduction band is the solid electric conductive. The lower band is called the valence band by similarity with the valence electrons of individual atoms. Both insulators and semiconductors have a band gap between the conduction band and the valence band. The difference is that the band gap in insulators is much larger and this is called forbidden band gap where it is difficult to excite electrons from their valence band to their conduction band. The present theory of the excitation of the electrons in valence band to conduction band is mainly due to thermal energy. For the photocatalysis reaction on semiconductors, the absorbed irradiation functions as thermal energy and excites the electrons from valence band to conduction band. Therefore, the width of band gap is one of the most important properties which strongly influence the electrical and optical properties of the material. Broader band gap needs more energy to excite the electrons which means only the irradiation carrying higher energy such as ultraviolet light and microwave can be used for the energy source during the reaction process. The irradiation with lower energy, visible light and infrared for example, can only drive catalysts with narrow band gap [44].

1.2.2 Mechanism of photocatalysis

In an ideal photocatalytic process, photocatalytic reactions were initiated by electron–hole pairs after bandgap excitation. Figure 1.3 show the schematic diagram of redox reaction occurred on the photocatalyst. When a semiconductor photocatalyst absorbs photon energy equivalent to or greater than the band gap energy of the photocatalyst, electrons in the valence band are excited into the conduction band, leaving a positive hole in the valence band. The photo–generated holes in the valence band can recombine with the photo–excited electron in the conduction band and dissipates the input energy as heat.

However, the electrons and holes can migrate to the catalyst surface, where they can participate in various oxidation and reduction reactions with absorbed other species present on the surface. In most case, the positive holes can react easily with surface bound water (H_2O) to from hydroxyl radicals ($\cdot OH$), whereas, the negative electrons can react with oxygen molecules (O_2) to form superoxide anion radicals ($\cdot O_2^-$). The $\cdot OH$ and $\cdot O_2^-$ are extremely strong, non–selective oxidant which lead to the complete mineralization of organics. Moreover, the high oxidative potential of the hole in the photocatalyst also allows the direct oxidation of organic matter to reactive intermediates. The $\cdot O_2^-$ was further protonated to from hydroperoxyl radicals ($\cdot OOH$) and subsequently hydrogen peroxide (H_2O_2). The $\cdot OOH$ also functions as electron scavengers to trap conduction band electrons which further defer the recombination process. The photocatalytic process can be expressed by the following equations [26–27, 45]:

$$\text{Photocatalyst} + h\nu \longrightarrow e^- + h^+$$

$$e^- + O_2\ \text{(adsorbed)} \longrightarrow \cdot O^{2-}$$

$$e^- + \cdot O^{2-} + 2H^+ \longrightarrow H_2O_2$$

$$e^- + H_2O_2 \longrightarrow \cdot OH + OH^-$$

$$h^+ + OH^- \longrightarrow \cdot OH$$

$$h^+ + H_2O\ \text{(adsorbed)} \longrightarrow \cdot OH + H^+$$

$$H^+ + \cdot O^{2-} \longrightarrow \cdot O_2H$$

$$H_2O + \cdot O^{2-} \longrightarrow OH^- + \cdot OOH$$

$$2\cdot O_2H \longrightarrow H_2O_2 + O_2$$

$$H_2O_2 + \cdot O_2^- \longrightarrow \cdot OH + O_2 + OH^-$$

$$(\cdot OH, \cdot O_2^-, \cdot O_2H) + \text{organic} \longrightarrow \text{degradation products}$$

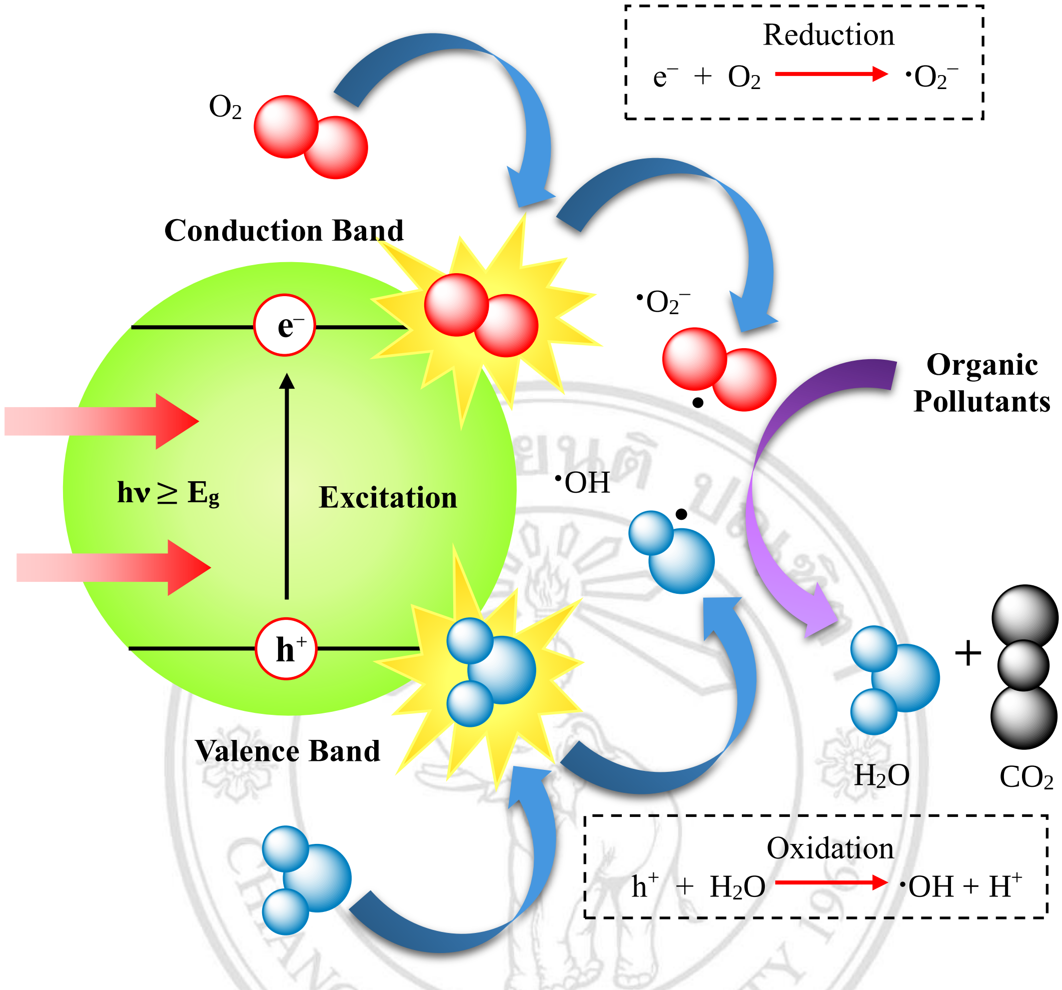

Figure 1.3 Photocatalytic redox reaction on semiconductor photocatalytic [45].

1.3 Synthesis

Nanomaterials can be synthesized either by breaking down the bulk material into smaller and smaller dimensions. The former is known as the “Bottom up” approach whereas the latter is referred to as the “Top down’ method (Figure 1.4). Many techniques including both Top–down and Bottom–up approaches have been developed and applied for the synthesis of the nanoparticles. In the Top–down approach a block of a bulk material is whittled or sculptured to get the nanosized particle. The Top–down approaches include milling or attrition, lithography etc. The main disadvantage of the Top–down approach is the imperfection of the surface structure. The nanoparticles produced by the attrition have a relatively broad size distribution and various particle shape or geometry. In addition they may contain significant amount of impurities. In the Bottom–up approach, the individual atoms and molecules are placed or self–assembled precisely where they are needed. Here, the molecule or atomic building blocks fit together to produce nanoparticles. Bottom–up approaches are more favorable and popular in the synthesis of nanoparticles and many preparation techniques of Bottom–up approach have been developed.

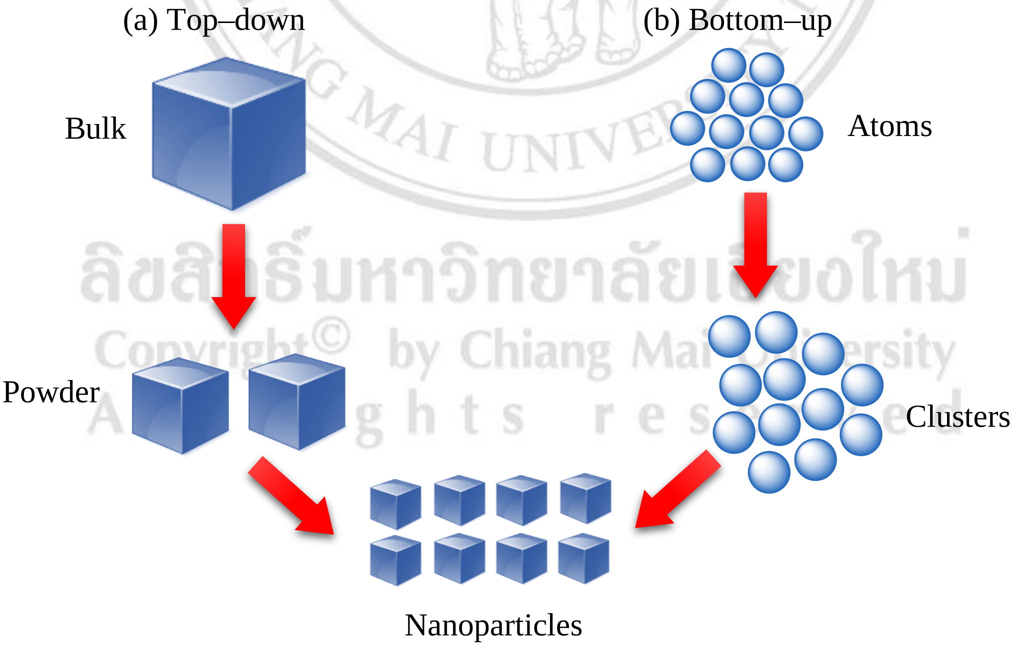

Figure 1.4 (a) Top down and (b) bottom up approaches in nanotechnology [46].

There are a number of conventional synthetic methods have been synthesized micro/nanomaterials with different shaped and sized. Most of the resultant materials were aggregated, non–uniform in size, required high reaction temperature and long reaction time. Thus, it is highly desirable to explore a low temperature, environmentally benign and convenient route for mass production of well disperse and uniform material. Microwave irradiation method is a relative new technique that provides many advantages over the conventional method. The microwave irradiation is a very efficient method in the selective heating of materials, as the energy can be transferred directly to the material. The volumetric constant is rapidly heated up to high temperature by microwave within a very short time. This results in less energy consumption, save in process–time, and is more environmental friendly. Moreover, it may create uniform products and reduce unwanted side reactions that normally occur in the conventional method. Thus, the microwave irradiation method is very high interesting because shape and size of the materials are able to be controlled with ease even at different synthetic conditions. In this research, microwave synthesis was chosen for the synthesis method of the materials.

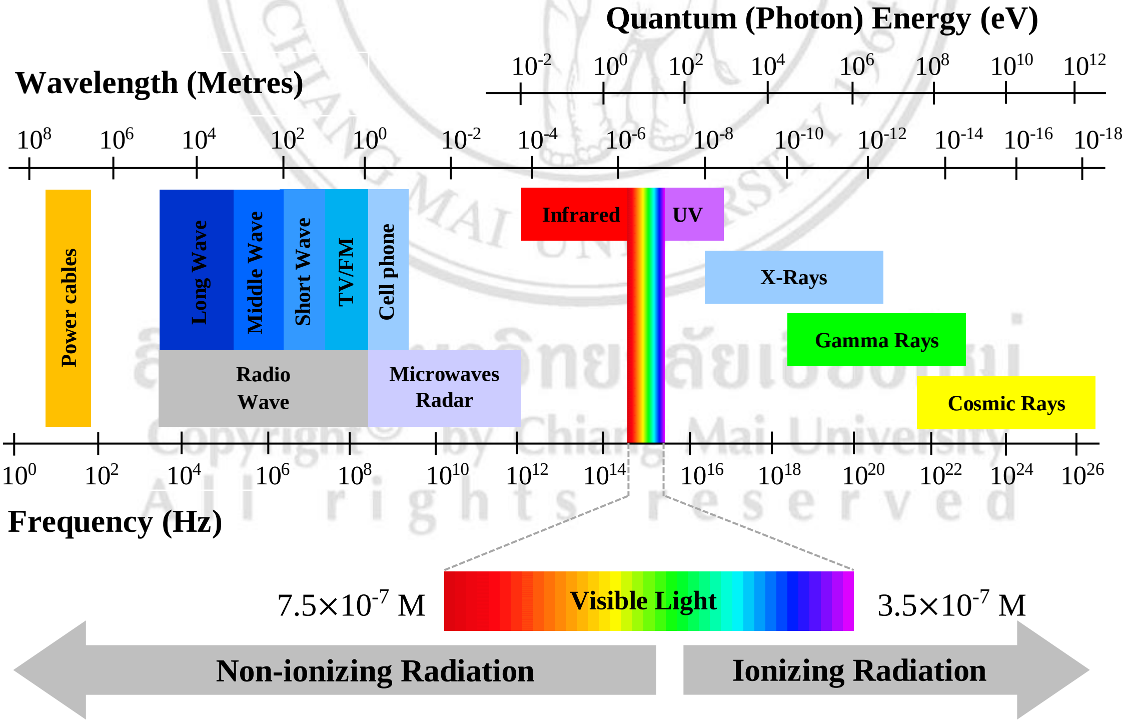

Figure 1.5 Electromagnetic waves spectrum [47].

Microwave irradiation is electromagnetic radiation in the frequency range 0.3 to 300 GHz, which corresponds to wavelengths of 1 mm to 1 m. In the electromagnetic spectrum, the microwaves region is located between infrared radiation and radio waves (Figure 1.5). However, for their use in laboratory reactions a frequency of 2.45 GHz is preferred. The energy of a microwave photon at 2.45 GHz is very low. The energy supplied is much too low to cleave molecule bonds. Microwave chemistry is based on the efficient heating of matter by microwave dielectric heating on the ability of a specific material to absorb microwave energy and to convert it into heat [48–49].

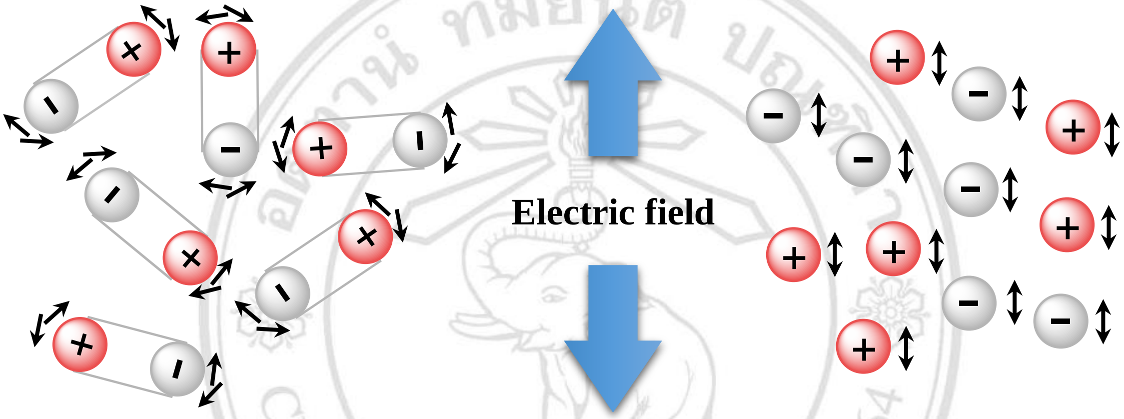

(a) Dipolar polarization (b) Ionic conduction

Figure 1.6 Schematic illustration of the two main dielectric heating mechanisms: (a) dipolar polarization (dipoles align in the microwave field) and (b) ionic conduction (ions move in the microwave field) [48].

The fundamental mechanism of microwave for transferring energy from microwaves to the substance being heat involves two main processes, namely dipolar polarization and ionic conduction. When the dipoles of irradiated molecules in solution try to follow the field and align themselves in phase with oscillating electric or magnetic field, they generate heat. The ability of this mechanism is related to the polarity of the molecules and their ability to align with the magnetic field. The key essential for dipolar polarization is that the frequency range of the oscillating field should be appropriate to enable sufficient inter–particle interaction. If the frequency range is very high, inter–molecules forces will stop the motion of a polar molecule before it tries to follow the field, resulting in insufficient inter–particle interaction. On the other hand, if the frequency range is low, the polar molecule gets enough time to align itself in phase with the field. Thus, no random interaction occurs between the adjoining particles. Microwave radiation has the appropriated frequency to oscillate polar particles and enable enough inter–particle interaction. This makes it an ideal choice for heating polar solutions. In the case of ionic conduction the dissolved charged particles oscillate back and forth under the influence of the microwave irradiation, colliding with neighboring molecules, and thus create heat. These collisions of ions with other species in solution generate much more heat than dipole polarization.

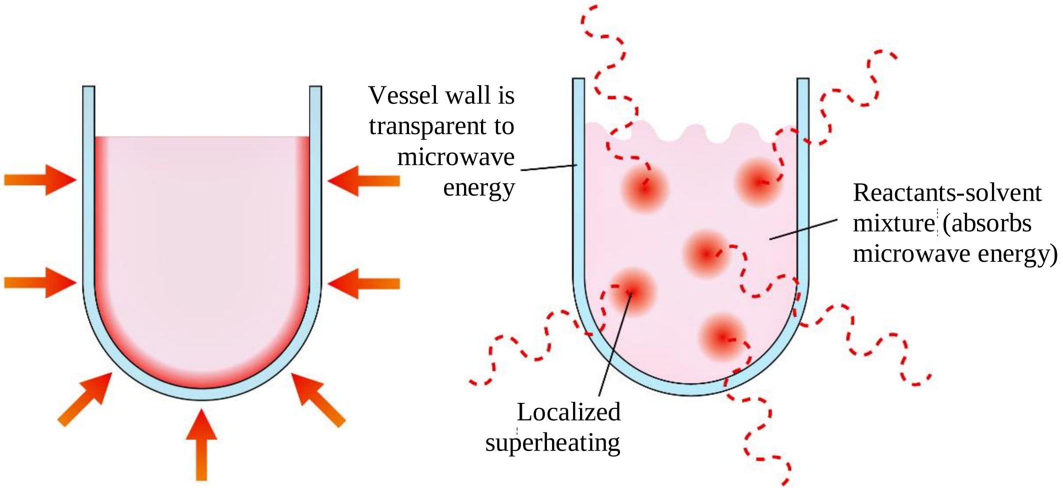

(a) Conventional heating (b) Microwave heating

Figure 1.7 Difference between (a) conventional heating and (b) microwave heating [50].

In the liquid phase preparation of nanoparticles most of the syntheses are achieved by a conventional external heat source which heat is driven into the substance passing, first though the wall of the vessel in order to reach to the solvent and reactants. This is slow and rather inefficient method for transferring energy into the reacting system because it depends on convection current and on the thermal conductivity of the various materials and substances that must be penetrated (Figure 1.7a). Microwave heating, on the other hand, produces efficient internal heating, increasing the temperature of the entire volume simultaneously and uniformly. As shown in Figure 1.7b, the microwave couple directly with the molecules of the whole reaction mixture which lead to rapid rise in the reaction temperature. This process is independent of material conductivity instantaneous localized superheating can be achieved. It is considered as the new synthetic route for chemical synthesis of metal nanoparticles.

1.4 Characterization Techniques

Several techniques such as X–ray diffraction (XRD), X–ray photoelectron spectroscopy (XPS), Fourier transform infrared spectroscopy (FTIR), Scanning electron microscopy (SEM), Transmission electron microscopy (TEM), Energy dispersive X–ray spectroscopy (EDX), Brunauer Emmett Teller (BET) method, Photoluminescence spectroscopy (PL) and UV–visible spectroscopy (UV–vis) have been widely used for determining the phase, morphology, atomic vibration, specific surface area and optical properties of nanoparticles.

1.5.1 X–ray diffraction (XRD)

Figure 1.8 X–ray diffraction spectrometer [51].

X–ray diffraction is a versatile analytical and non–destructive technique with practical applications in a wide range of materials science. The crystalline and amorphous structure of nano–materials have been conventionally studied by XRD. The XRD method is based on the ability of crystals to diffract X–rays in characterize manner allowing an accurate study of the structure of crystalline phase. However, the crystalline materials are characterized by a periodic arrangement of atoms identified. When irradiated with X–rays of fixed wavelengths, the electrons of atoms in the crystal interact with the radiation and undergo an elastic collision to make them oscillate. The electron surrounding the atomic nuclei becomes secondary sources to create a coherent source of electromagnetic radiation at the same frequency and phase as that of the incoming X–ray. The wave emitted from different atoms will undergo constructive or destructive interference. Constructive wave interference follows Braggs' law, while destructive interference disobeys the same. The process is schematically shown in Figure 1.9, where the sample is exposed to an disclosed to an X–ray beam of wavelength (λ) at an angle θ with the tangential surface, which undergoes diffraction and detected at an angle of 2θ represented as equation here,

$$n\lambda = 2d_{hkl}\sin\theta \tag{1.1}$$

where, n is the order of diffraction, λ is the wavelength of the incident beam in nm, d_{hkl} is the lattice spacing of the diffracting *hkl* plane and θ is the angle of scattering.

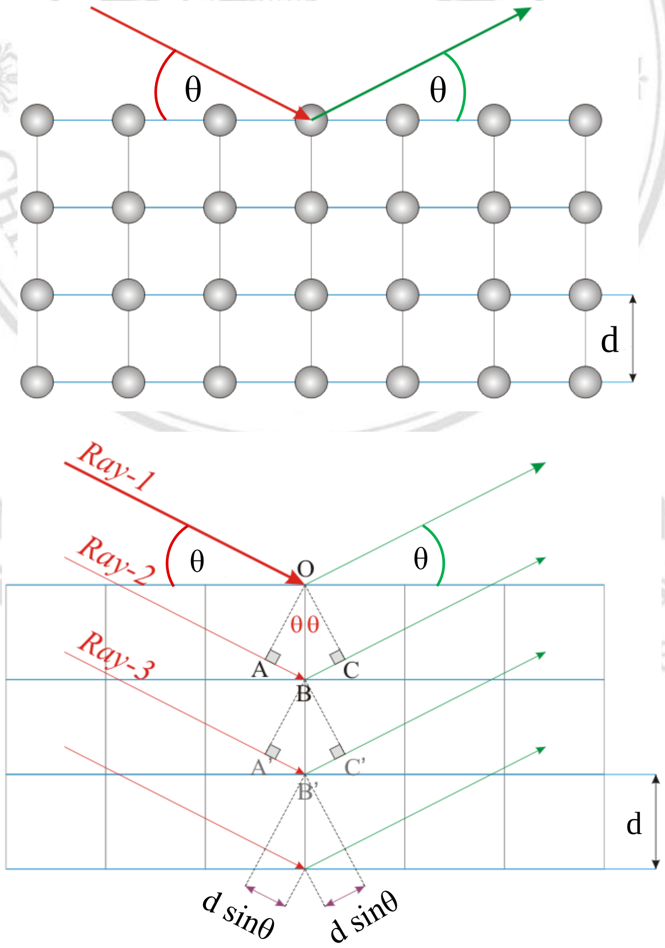

Figure 1.9 Geometry for interference of a wave scattered from two planes separated by a spacing, d [52].

The diffraction pattern generated contains information on the crystallographic structure, atomic positions, chemical composition, and degree of crystallinity or amorphous content and crystalline size/strain. The average crystalline size is determined form XRD pattern with the help of the Debye–Scherrer equation,

$$D = K\lambda/\beta \cos\theta \tag{1.2}$$

where, D is the thickness of the crystal, K is the shape factor depending on the Miller index of the reflecting plane and the shape of the crystal, λ is the wavelength of the X–rays, β is the full width at half maximum (FWHM) of the diffraction peak and θ is the Bragg angle of the peak. The width of the peaks in detail phase pattern provides an indication of the average crystalline size. Large crystallites give rise to shape peaks, as the crystallite size reduces, the peak width increases and the intensity decreases. Crystallite size does not equal the size of the particle as one particle can be a conglomerate of several crystallites. Peak broadening can also occurs from variations in lattice spacing, caused by lattice strain. Moreover, this technique has the great advantage that no sample preparation, in comparison to other techniques. The polycrystalline solid samples and even liquids can be either in the form of thin foil, compact flat pack and a glass capillary [52, 53].

1.5.2 X–ray photoelectron spectroscopy (XPS)

Figure 1.10 X–ray photoelectron spectrometer [54].

X–ray photoelectron spectroscopy is the most widely technique for analyzing the surface composition of materials in different chemical environments. XPS can measure the elemental composition, empirical formula, chemical state and electronic state of surface and interface that influence properties of nanostructured materials. XPS spectra are obtained by irradiating a solid surface with a beam of monoenergetic photons. The photons have certain energy that when they interact electrons in the atoms of the material with the energy necessary the electrons from the atoms in the material are ejected from the atom. The electrons ejected are detected in the XPS detector by measuring electrons kinetic energy which provides the information to determine the kind of elements present in the material figure 1.11 illustrates the schematic representation of the X–ray photoelectron process.

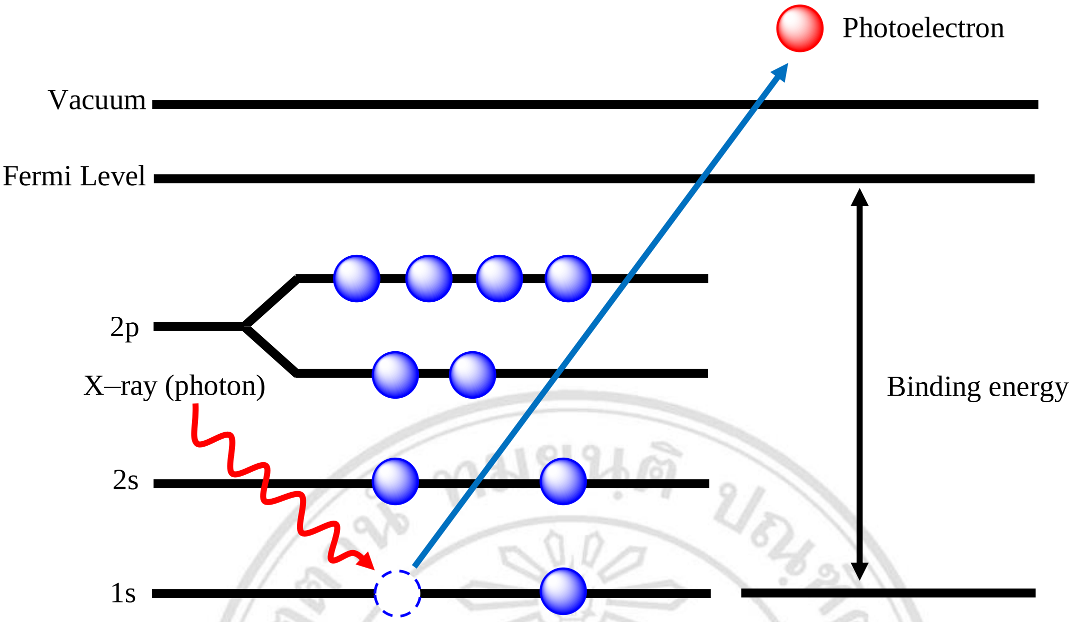

Figure 1.11 Schematic representation of the X–ray photoelectron process [55].

The photoelectron kinetic energy is named E_k and it is measured quantity in the experiment, is given by Einstein's relationship,

$$E_k = h\nu - E_b \qquad (1.3)$$

Where hν is the energy of a photon and E_b is the binding energy of the electron in a particular level. If the incident photon is sufficiently energetic, many different levels in the sample may be ionized and thus a spectra is generated showing all accessible energy levels as a distribution of photoelectrons with kinetic energies dominated by equation [55–57].

1.5.3 Fourier transform infrared (FTIR) spectroscopy

Figure 1.12 Fourier transform infrared spectrometer [58].

Fourier transform infrared (FTIR) spectroscopy is today one of the most important analytical techniques available to scientists. FTIR is a physical and chemical method based on measurement of vibration of the atoms of a molecule excited by IR radiation at specific wavelength range. However, the middle infrared region between 4000–400 cm^{-1} is the most attractive for chemical analysis. As IR radiation is passed through a sample, specific wavelengths are absorbed causing the chemical bonds in the material to undergo vibrations such as stretching, contracting, and bending. Functional groups present in a molecule structure tend to absorb IR radiation in the same wavenumber range regardless of other structures in the molecule, and spectral peaks are derived from the absorption of bond vibrational energy changes in the IR region. Thus there is a correlation between IR peak positions and chemical structures in the molecule. In addition to providing qualitative information about functional groups, IR spectra can provide quantitative information of every different kind of material. It is extremely accurate, rapid and inexpensive method for analysis of solids that are crystalline, microcrystalline, amorphous, or films. Thus, it a very reliable technique for identification of virtually any sample [59].

FTIR spectrometers may be either single or double beam producing a transmittance spectrum. Most systems multiply the transmittance value by 100, to give percent transmittance (T). However, the absorbance (A) scale, where $A = -\ln(T/100)$, is more and more used for quantitative analysis, following Beer’s law that there is a linear relationship between absorbance and sample concentration [60]. Here the sample is dispersed, in KBr, at a sample/KBr ratio of about 1% and pressed into a disc. Discs may be heated above overnight to remove absorbed water, whose IR bands can overlap with those of the sample.

1.5.4 Scanning electron microscopy (SEM)

Figure 1.13 Scanning electron microscope [61].

Scanning electron microscopy is certainly one of the most important analytical techniques available to today’s scientists. SEM can provide information on surface topography, morphology, crystalline structure and chemical composition of the specimen at very high resolution. The main composition of typical SEM are electron optical system scanning system, detector, display, vacuum system and electronic controls. The electron optical system consists of an electron gun, a condenser lens and an objective lens operating in vacuum. A fine electron probe, with a spot size less than 10 nm in diameter, is generated by focusing electrons emitting from an electron gun on to surface of the specimen using a series of electromagnetic lens and scanning coil. Each point on the specimen that is struck by the accelerated electrons emits signal in the form of electromagnetic radiation. Selected portions of this radiation are collected by a detector and the output signal is amplified and then transferred to the displayed unit. The type of signals produced by a SEM include secondary electrons (SE) and back–scattered electrons (BSE). The resulting image is generally straightforward to interpret, at least for topographic imaging of objects at low magnifications [62–63].

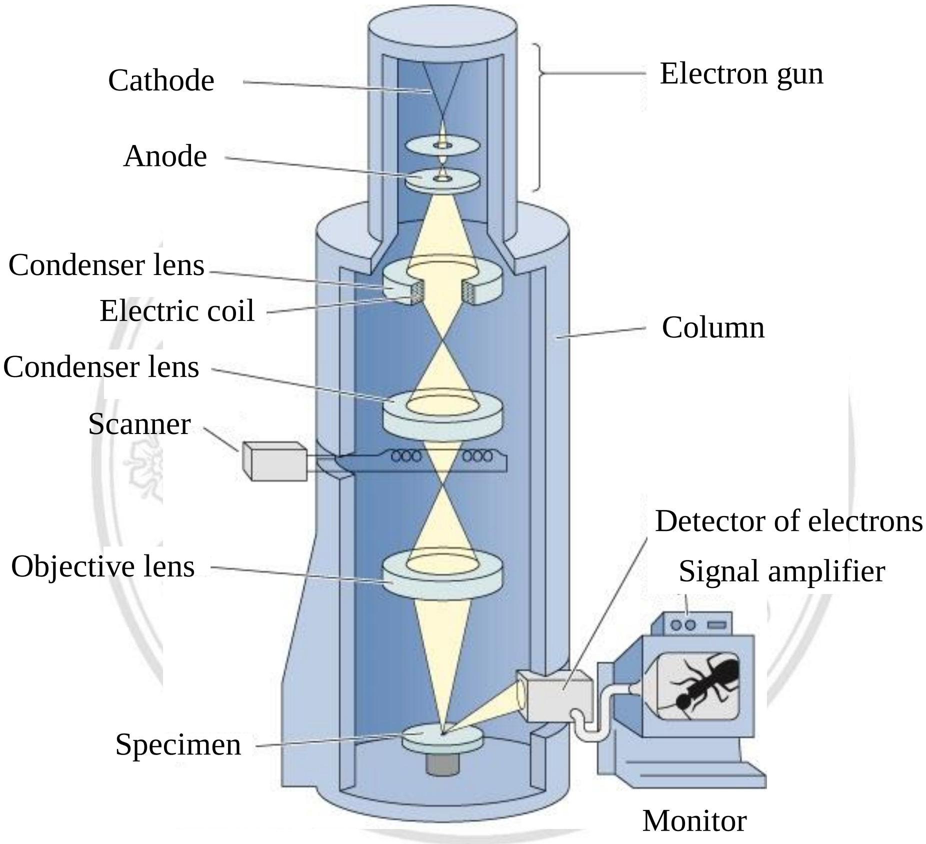

Figure 1.14 Schematic diagram of scanning electron microscope [64].

1.5.5 Transmission electron microscopy (TEM)

Figure 1.15 Transmission electron microscope [65].

Transmission electron microscopy is an established technique for investigating the crystal and the structure of nanophase materials. It is used to study all varieties of solid materials metal, semiconductor, polymers and composites. It can provide morphological information of size and shape of phases in micro/nanostructure and chemical composition. Moreover the aforementioned information, it can display the nature of crystallographic defects. With the TEM mainly all incoming electrons are transmitted through a specimen that is appropriately thin. Moreover, electron may be scattered by the atom of the specimen. The electrons used in a TEM are capable of penetrating many atomic planes and so are diffracted by crystalline regions of materials. Their wavelength is much less than a typical atomic–spacing so that according to the Bragg equation $n\lambda = 2d_{hkl} \sin\theta$. Diffraction shows elastic scattering of electrons in crystal. The regularity of the spacing of these nuclei results in a redistribution of the angular distribution of the scattered intensity. Instead of continuous distribution over scattering angle, there are shape peaks centered around certain scattering angles, each twice the corresponding Bragg angle θ. In the TEM this angular distribution can be displayed by magnifying the diffraction pattern first formed at the back focal of the objective lens. Examination of the TEM image of the polycrystalline specimen shows that there is a variation of electron intensity within each crystallite. This diffraction contrast arises either from atomic defects within the crystalline or the crystalline nature of the materials itself, combined with the wave nature of transmitted electrons.

The resolution of the TEM could be improved by particular arrangements of the magnetic fields serving as focuses of the electron beam, by enhancing the energy of the electrons. The major advantage of the HREM are the direct observations of the detailed nanostructures, such as the core/shell structure, the interfaces and the surfaces, the atomic defects the twin structures etc. The nanocrystal characterization can be done using transmission microscopy. Here, an electron beam is used to image a thin sample in transmission mode. The resolution is a sensitive function of the beam voltage and electron optics: a low–resolution microscope operating at 100 kV might have a 2–3 Å resolution while a high voltage machine designed for imaging can have a resolution approaching 1 Å. Since nanocrystalline samples range from ten to hundreds of angstroms in size, this type of microscopy allows both the interior crystal structure and the overall particle shape to be measured. A single TEM picture of a nanocrystalline sample can provide an enormous amount of information. Low resolution TEM can also be used to determine sample distributions and shapes. Higher resolution images show the discrete nature of the crystalline interior of nanoparticles and can detect the presence of certain crystalline defects; the Fourier transform of such images provides a measure of the lattice spacing and crystallographic parameters. More sophisticated analysis of high–resolution TEM images can provide even deeper insight into subtle structural aspects of nanocrystals. Simulation of high–resolution images can, in principle, provide data concerning whether the average bond length in a nanocrystals is uniform or variable within the nanocrystals interior. Another exciting prospect is the use of TEM to give direct information about nanocrystals surfaces including reconstructions and dynamic motions of atoms at surfaces. Thus the TEM image gives information about the particle shape, size and size distribution [66–67].

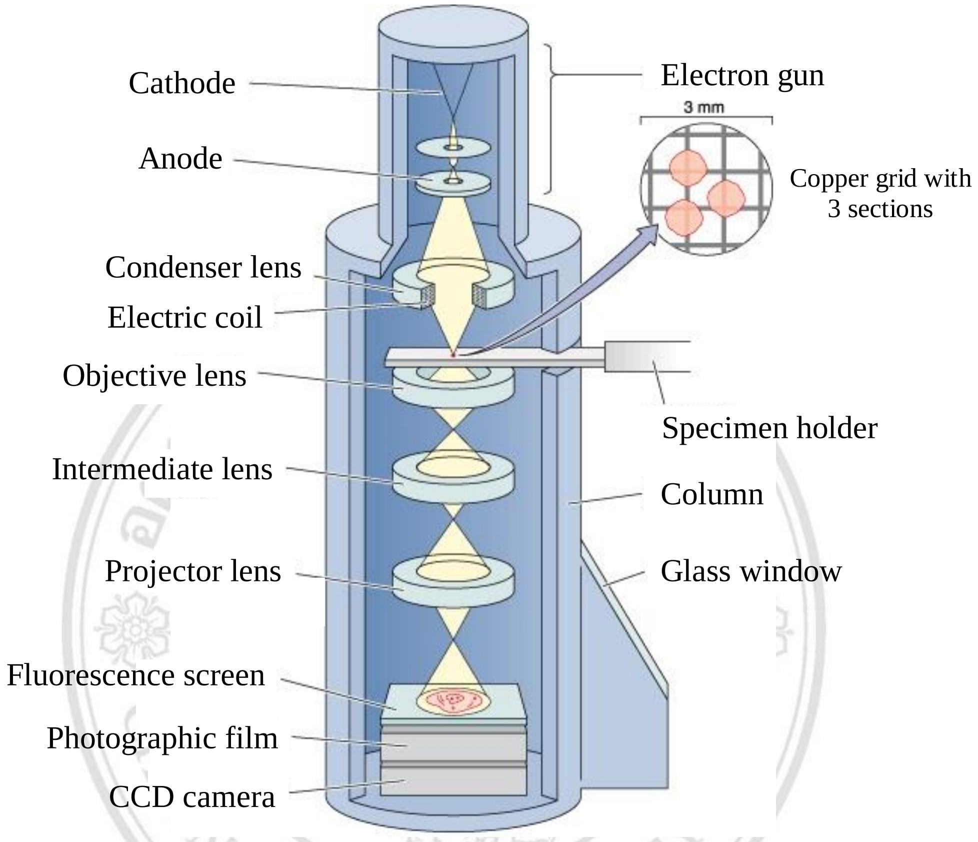

Figure 1.16 Schematic diagram of transmission electron microscope [68].

1.5.6 Surface area analyzers

Figure 1.17 Surface area analyzers [69].

The specific surface area of the solid is the summation of the areas of the disclosed surfaces of the particles per units mass. There cannot be calculated from particle size information, but is defined at the atomic level by the physical adsorption of a vapor or gas onto the surface of a solid. Brunauer, Emmett and Teller (BET) gas adsorption is the commonly model used to determine the total surface area of fine powders and porous materials. The BET derived an isotherm for the adsorption of multimolecular layers of gas on a solid adsorbent according to the Langmuir model a unimolecular layer. Samples are prepared by heating while concurrently flowing gas over the sample to remove the released impurities. The prepared samples are then cooled, under vacuum with liquid nitrogen and analyzed by measuring the amount of gas adsorbed at specific pressures [70].

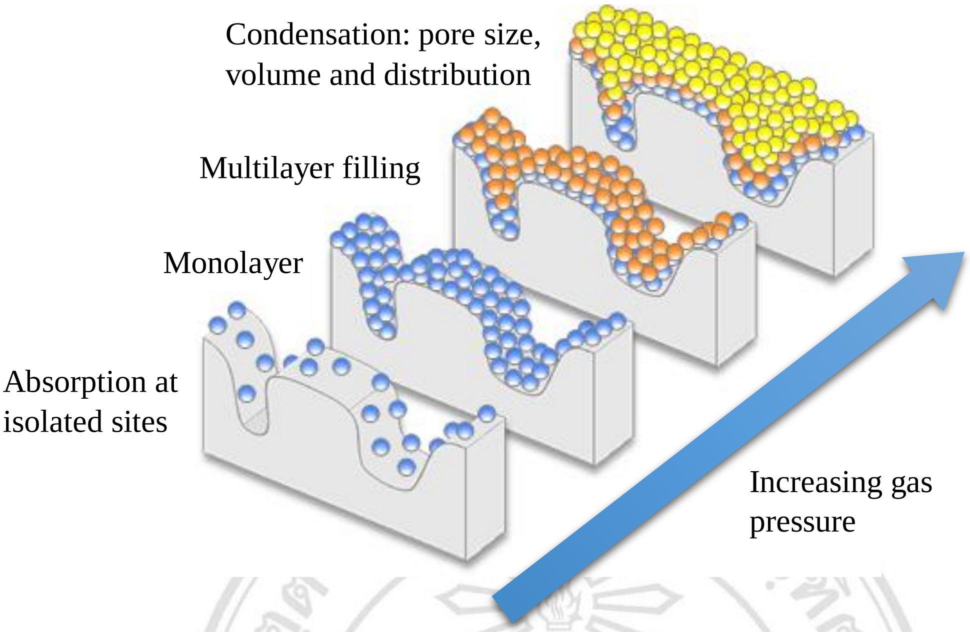

Figure 1.18 Schematic of the adsorption of gas molecules onto the surface of a sample showing the monolayer adsorption model assumed by the Langmuir theory and the multilayer adsorption model assumed by the BET theory [71].

1.5.6 Photoluminescence (PL) spectroscopy

Figure 1.19 Photoluminescence spectrometer [72].

Photoluminescence spectroscopy is one of the most essential technique to the investigation of the electronic structures and optical properties of semiconductor materials because it is a nondestructive method and normally it does not require any special sample preparation. The emission of light from a semiconductor material is studied under optical excitation with an energy greater than the band gap energy of the studied materials. During a PL spectroscopy experiment, excitation is provided by laser light with an energy much larger than the optical bandgap. The photo–excited carriers compose of electrons and holes, which relax toward their respective band edges and recombine by emitting light at the energy of the bandgap. But, radiative transitions in semiconductors may also involve localized defects or impurity levels. Thus, the PL emission spectrum can be used identify specific defects or impurities, and the magnitude of the PL signal allows determining their concentration. Moreover, the emission spectrum can give information about bandgap, exciton states, and confinement energy of semiconductor and other functional materials [73–74].

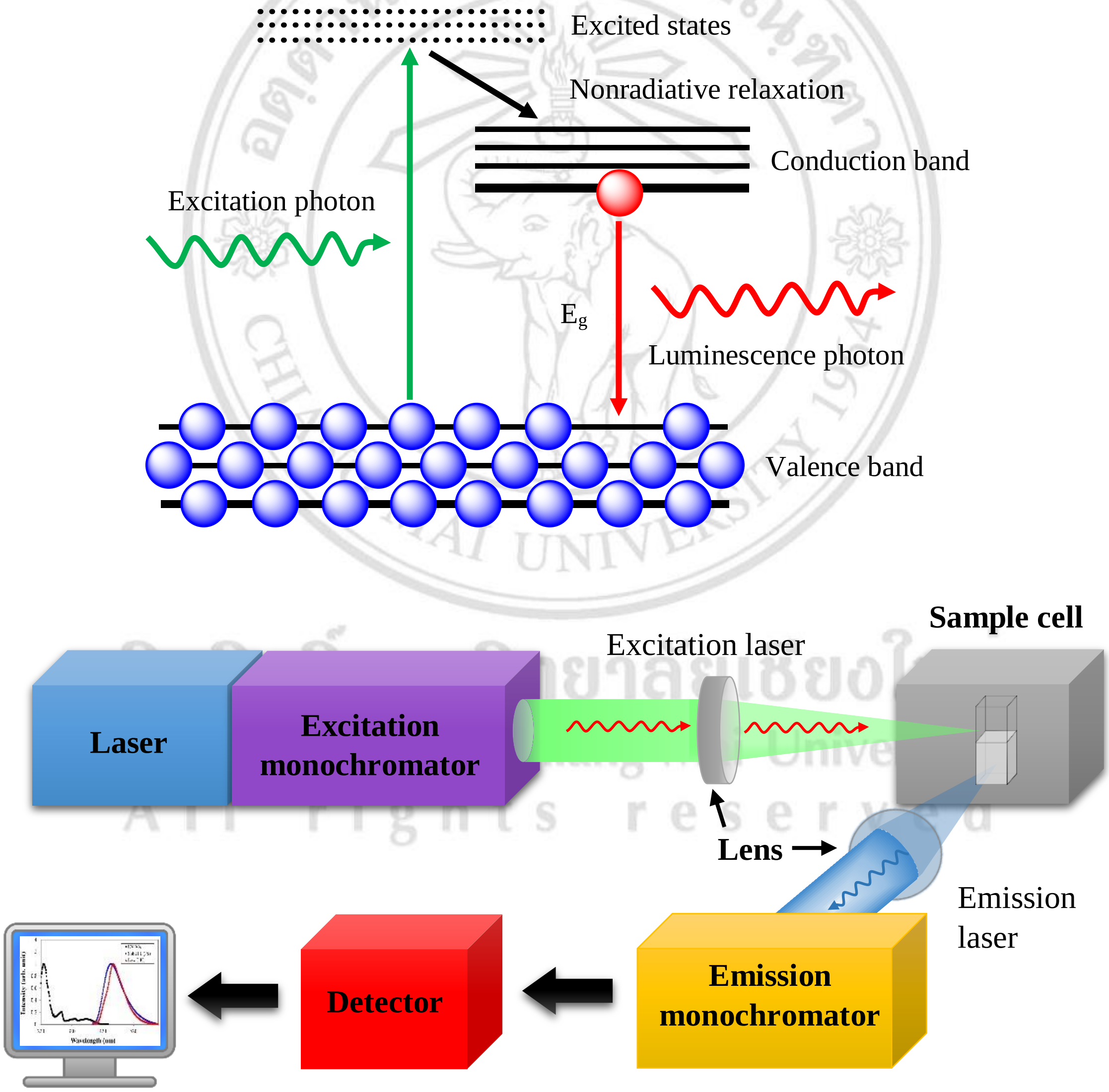

Figure 1.20 Schematic diagram of photoluminescence spectrometer [75].

1.5.7 UV–visible spectroscopy

Figure 1.21 UV–visible spectrometer [76].

UV–visible spectroscopy is a technique used to measure the absorption, transmission and emission of ultraviolet and visible light wavelengths by a substance in solution. This technique is widely use to study the electronic structure, chemical environment for monitoring the progress of reactions and the quantitative analysis. A molecule or ion will display absorption in the ultraviolet or visible region when radiation causes an electronic transition within its structure. It commonly provides the information about the changes in electronic energy levels within of the molecule or atom arising due to transfer of electron from lower energy level (a less excited state or the ground state) to higher energy levels (an excited state). A spectrophotometer is commonly consist of a light source, a sample holder, a diffraction grating in a monochromator or a wavelength selector, a sample containers, a photoelectric detector, and signal processor and readout. The containers of the sample and reference solution are made by on optically materials such as glass, plastic and silica. Glass and plastic containers are also common, although glass and almost plastics absorb in the UV, which limits their usefulness to visible wavelengths. The light source is generally a Tungsten–halogen lamp, a deuterium arc lamp, a xenon arc lamp. A monochromator composes of an entrance slit, a collimating lens, a dispersing device, a focusing lens and an exit slit. Theoretically, the output from monochromator is monochromatic light. A spectrometer can be either single beam or double beam. The single beam instrument has a monochromator between the source and the sample to analyze one wavelength at a time. The double beam instrument has a single source and a monochromator and then there is a splitter and a series of mirrors to get the beam to a reference sample and the sample to be analyzed, this allows for more accurate monochromator between the sample and the source; instead, it has a diode array detector that allows the instrument to simultaneously detect the absorbance at all wavelengths. The basic principle of this type of spectroscopy composes of that light of definite interval of wavelength passes through the solution of a sample in the container and falls on to the photoelectric cell that transforms the radiant energy into electrical energy measured by a galvanometer. The schematic representation of UV–visible spectrometer is shown in figure.

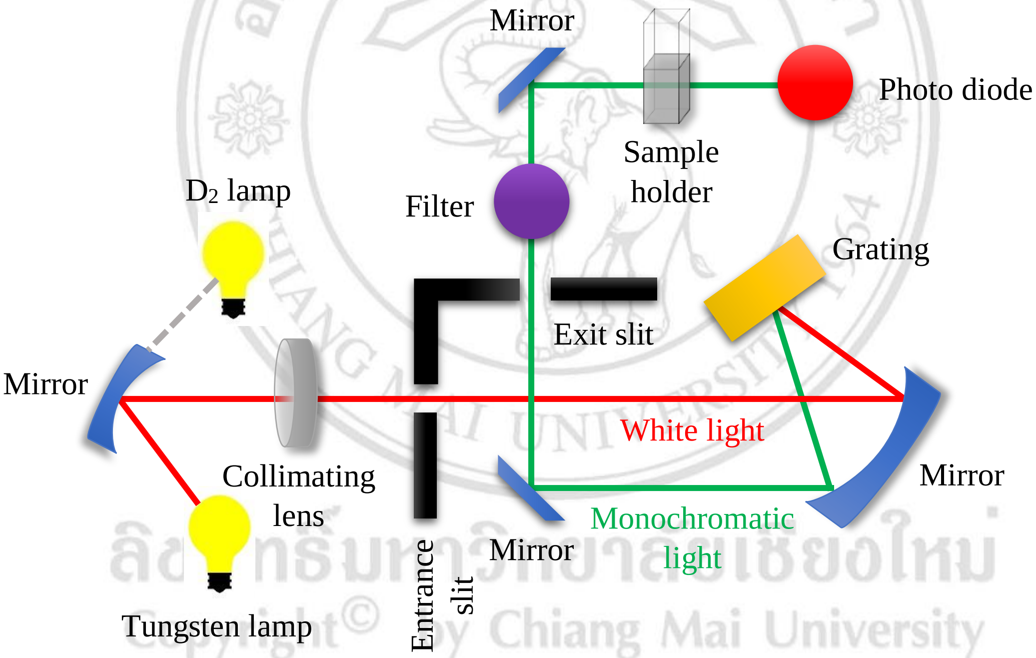

(a) Single beam

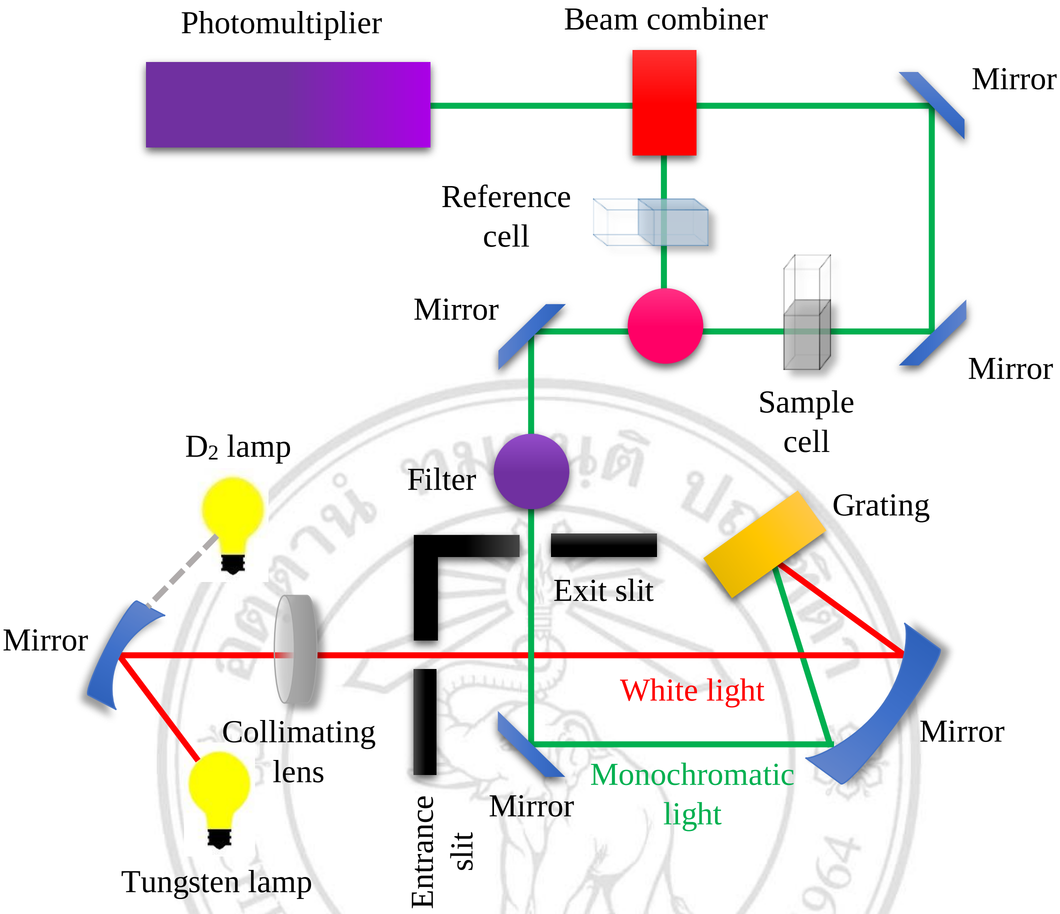

(b) Double beam

Figure 1.22 Schematic diagram showing a single beam (a) and a double beam (b) spectrophotometer [77].

When monochromatic radiation passes through the solution of sample in the container, the intensity of the emitted radiation depends upon the thickness and the concentration of the solution. I_o is the intensity of light illuminating the sample and I is the intensity of light transmitted through the sample. The ratio of these intensities is the transmittance, T, which is defined according to the formula:

$$T = I/I_0 \tag{1.4}$$

This is sometimes expressed as a percentage and referred to as %transmittance. Mathematically, the absorbance is related to percentage transmittance by the expression:

$$A = -\log T = -\log(I / I_o) = \log(I_o / I) \tag{1.5}$$

The Beer–Lambert Law describes the relationship between absorbance and concentration, which verifies that the absorbance of a solution is directly proportional to the concentration of the analyte. Beer's Law can be written as well as,

$$A = \varepsilon bc \tag{1.6}$$

, where A is absorbance, ε is the extinction coefficient, b is the sample path length, and c is the sample concentration [78].

Furthermore, the optical band gap (E_g) of semiconducting materials can be calculated via UV–vis spectroscopy using absorption edge values from absorption spectra. The optical absorption can be calculated according to the Tauc's formula by the following equation as follows [79]:

$$(\alpha h\nu) = B(h\nu - E_g)^n \tag{1.7}$$

, where α is an absorption coefficient, ν is a photonic frequency, h is the Planck' s constant, B is a constant, and E_g is a band gap energy controlled by electronegativity, crystalline degree, defects and others and n is the integer related to the characteristics of the optical transition which assumes the values n = 1/2 for allowed direct transition, n = 3/2 for direct forbidden transition, n = 2 for allowed indirect transition and n = 3 for indirect forbidden transition

1.5 Literature Review

ZHS has been widely used as a nontoxic flame–retardant and smoke–suppressant additive for many polymeric materials**,** due to its economical, safety, and high effective flame– and smoke– retardant properties [13–15]. Some other potential applications of ZHS were also developed in recent years: using as a gas sensor for formaldehyde, ethanol and carbon monoxide (CO) detection [19, 80–82] and as photocatalysts to degrade organic pollutants. Among them, one of the most promising applications is photocatalysis. Recently, ZHS has been reported to exhibit certain photocatalytic activity for degradation of gaseous benzene (C_6H_6) [11, 26, 28, 34], a typical and major indoor air pollutant, and photocatalytic reforming of ethanol to H_2 and CH_4 [25]. Some other photocatalytic activities of ZHS, including degradation of methyl orange [12, 26] and cyclohexane [12] are also motivation by these works. In addition, ZHS thermal decomposition products including $ZnSnO_3$ and Zn_2SnO_4/SnO_2 mixtures could also be applied to solar cells [21], lithium ion battery anodes [16–18], gas sensors [20] and photocatalysts [23]. Considering the aforementioned applications, ZHS has been prepared via several different methods such as grinding, co–precipitation, sonochemical, hydrothermal [23–30] and solvothermal reactions.

Zang *et al.* [30] reported the growth of zinc hydoxystannate microcubes on a thin film of pre-synthesized ZnO nanoparticles served as the source of Zn for the hydrothermal growth. The reaction was carried out in a Teflon–lined autoclave at 120 ºC by dipping the substrate coated with ZnO nanoparticles in a solution of $SnCl_4$. The structures and morphology of the as–prepared ZHS microcubes were characterized by X–ray diffraction (XRD), scanning electron microscope (SEM) and transmission electron microscope (TEM). The microcubes were single phase cubic perovskite crystalline structure. Both the concentration of the $Sn(OH)_6^{2-}$ ions and the molar ratio of NaOH to $SnCl_2$ are found to play the important roles in determining size and shape of the ZHS crystalline phase.

Fu *et al.* [11] successfully fabricated ZHS particles by solvothermal process, using $ZnCl_2$ and $SnCl_4·5H_2O$ as starting reactant materials and ethylene glycol as solvent. X–ray diffraction (XRD), scanning electron microscope (SEM) and transmission electron microscope (TEM) results showed a pure cubic phase of ZHS. The band gap determined from the UV–visible spectrum was found to be 4.3 eV. Photocatalytic activity of the ZHS products for benzene degradation was systematically investigated under UV radiation. It was found that the ZHS nanoparticles showed very high activity for benzene degradation due to the abundance of surface OH groups which accept photogenerated holes to yield highly reactive OH radicals.

Qin *et al.* [29] prepared ZHS by ultrasonic treatment and the subsequent aging process in aqueous solution. The stoichiometric solution of $Zn(Ac)_2$ and $SnCl_4 \cdot 5H_2O$ was mixed with Na_2CO_3 to afford the precursor. X–ray diffraction pattern of the ZHS showed high crystalline structure. The synthesis procedure can proceed at low temperature without any organic solvents, showing that this method is facile and eco–friendly to produce well–dispersed and uniform ZHS submicrocubes with perfect shape.

The hydrothermal growth of zinc hydroxystannate micro/nano structures in aqueous mixture of zinc salt (zinc nitrate, zinc chloride, zinc sulfate, etc.) and stannic chloride was reported. The mixture is then reduced by sodium hydroxide at 130–180 ºC under high pressure in a sealed autoclave. Chen *et al.* [26] succeeded in synthesizing of nano–sized ZHS particles from the reaction of $ZnCl_2$ and $SnCl_4 \cdot 5H_2O$ via simple homogeneous precipitation comparing to the hydrothermal method without any template, catalysts, surfactants or organic solvents. The structure and morphology of the ZHS products were characterized by X–ray diffraction (XRD), scanning electron microscopy (SEM), transmission electron microscopy (TEM), ultraviolet–visible (UV–Vis) diffuse reflectance spectroscopy, and volumetric adsorption method (BET). The photocatalytic activity of the ZHS products for degradation of methyl orange and benzene was systematically investigated under UV radiation. They were found that ZHS synthesized by homogeneous precipitation method has higher activity for the degradation of methyl orange and benzene under UV radiation than those synthesized from the hydrothermal route.

Fu *et al.* [12] investigated the effect of preparation method, including grinding, co–precipitation, self–templating and hydrothermal processes on the microstructures and the photocatalytic performances of ZHS. The results were revealed by X–ray diffraction (XRD) and Fourier transform infrared (FTIR) spectroscopy. The morphology results showed the sample with less impact by the preparation method. Due to the susceptible of OH group, the surface microstructure and the photocatalytic performance are sensitive to the preparation methods. They were found that ZHS prepared by the PVP–assisted hydrothermal method exhibits the highest thermal stability, optical adsorption, BET surface area, and ability of activation of O_2, which were the consequent results in the highest photocatalytic activity and stability for the degradation of methyl orange.

1.6 Research Objectives

1.7.1 To synthesize of ZHS nanomaterials by novel simple microwave radiation, which are benign to the environment.

1.7.2 To study the parameter of synthetic conditions, such as pH of the solution and length of processing time which influence the phase purity, size and shape of the products.

1.7.3 To study the optical properties of the as–synthesized products and apply them as semiconducting materials for photocatalytic application under UV–visible light.

1.7 Usefulness of the Research (Theoretical and/or Applied)

1.8.1 The synthetic technique and condition are able to apply other large scale productions that can reduce production cost.

1.8.2 The ZHS compound is very useful for photocatalysis for waste water treatment, gas sensing nanomaterials and many others.